Length, Strength, Extensibility, and Thermal Stability of a Au−Au Bond in the Gold Monatomic Chain

Chang Q. Sun,*,† H. L. Bai,‡ S. Li,† B. K. Tay,† C. Li,† T. P. Chen,† and E. Y. Jiang‡

School of Electrical and Electronic Engineering, Nanyang Technological University, Singapore 639798, and Institute of Advanced Materials Physics and Faculty of Science, Tianjin University, Tianjin 30072, People's Republic of China

Received: June 26, 2003; In Final Form: December 2, 2003

Simulating the measured size dependence of both the E_{4f} level shift and the melting-point suppression of Au nanosolids reveals that (i) the E_{4f} core-level energy of an isolated Au atom is estimated to be −81.50 eV and the E_{4f} binding energy is −2.87 eV and (ii) the melting point of the Au monatomic chain (MC) is around 320 K, about 1/4.2 times the bulk value (1337.33 K). These intriguing changes are attributed to the effect of atomic coordination imperfection. An analytical solution has been derived showing that the maximal strain of a metallic bond in a MC under tensile stress varies inapparently with the mechanical stress but apparently with temperature in the form of $\exp[A/(T_m - 4.2T)]$, where A is a constant and T_m is the bulk melting point. Matching calculations to all the insofar-measured breaking limits (at 4 K, it is around 0.23 nm, and in the vicinity of room temperature, it is 0.29−0.48 nm) indicates that the measured divergent values originate from thermal and mechanical fluctuation near the melting point of the MC.

I. Introduction

Metallic nanosolids and metallic monatomic chains (MCs) have attracted tremendous interest, since they show intriguing properties from a basic scientific viewpoint, as well as great potential in upcoming technological applications such as nanoelectronic devices. The intriguing phenomena include quantum conductance, higher chemical reactivity, lower thermal stability, and the unusual mechanical strength and ductility. A metallic MC is an ideal prototype of nanowires for extensibility study, as the MC extension involves only bond stretching without atomic gliding dislocations as do atoms in metallic nanowires.[1] On the other hand, quantifying the intensity of crystal-binding intensity to a core electron of an isolated atom and its energy shift upon bulk and nanosolid formation is also a great challenge.[2,3] Although the quantum conductance is theoretically well understood due to the enlarged sublevel separation in the conduction band,[4,5] knowledge about the equilibrium bond length, bond strength, extensibility, and thermal and chemical stability of the MCs as well as the electronic structure of atoms in the MCs has not yet been consistent and satisfactory. The stretching limit of the Au−Au distance in the Au MC has been measured using transmission electron microscopy at room temperature to vary from 0.29 nm,[6] 0.36 nm (±30%),[7] 0.35−0.40 nm,[4] and even to a single event of 0.48 nm.[8] However, at 4.2 K, the breaking limit of the same Au−Au bond is reduced to 0.23 ± 0.04 nm as measured using scanning tunneling microscopy and to 0.26 ± 0.04 nm as measured using mechanically controllable break junctions[9] with respect to the bulk value of 0.2878 nm. Sophisticated density functional theory calculation[10] suggests that the pairwise potential applies, the Au−Au equilibrium distance (without external stimulus) is between 0.232 and 0.262 nm, and the cohesive energy per bond changes from −0.51 to −1.59 eV. The similar trends also hold for other metallic MCs such as Pt, Cu, and Ag in calculations. Unfortunately, numeral calculations for pure Au−MC have yielded a maximum Au−Au distance of 0.31 nm under tension,[11] which is inconsistent with the values measured at room temperature in an ultrahigh vacuum. According to calculations,[12] the mechanical strength of the Au−Au bond is about twice that of the bulk value. The measured distances between Au−Au atoms could not be theoretically solved unless light atoms such as X (H, B, C, N, O, and S) are inserted into the Au−Au chain in calculations. The light-atom insertion has led to gold separation in Au−X−Au that could finally match various observed Au−Au distances. For instance, the insertion of a carbon atom led to the stretched Au−C−Au distance of 0.39 nm just before breaking; wires containing B, N, and O displayed even larger distances when stretched. The Au−H−Au distance, 0.36 nm, agrees with one of the experimentally measured values, and the anomalously large distance of 0.48 nm matches the separation between gold atoms in an Au−S−Au chain.[13] Actually, it may not be easy for an H atom to bond more than one other atom. For instance, adding a H atom to a surface can terminate the (such as Si) surface bond ideally; diffusion of a H atom into a metal embrittles the metal substantially.[14] More than two atoms are required for C, N, and O to form a stable tetrahedron upon reaction due to their intrinsic valance states and orbital hybridization.[15] Furthermore, intensive experimental investigations[16,17] show that Au atoms could hardly bond to carbon atoms and thus make the Au-coated carbon nanotubes impossible. Oxygen-attacked corrosion should break or burn the MC or even the carbon nanotubes at a temperature that is much lower than the melting point (T_m), instead.[18,19] Therefore, impurity-modulated Au MC breaking limits may need further experimental confirmation. Besides the density functional theory approaches, Jiang et al.[20] correlated the formation tendency of

* Author to whom correspondence may be addressed. E-mail: ecqsun@ntu.edu.sg. Fax: 65 6792 0415. http://www.ntu.edu.sg/home/ecqsun/.
† Nanyang Technological University.
‡ Tianjin University.

10.1021/jp035815j CCC: $27.50
Published on Web 01/21/2004

a MC under tensile stress to the ratio between Peierls stress of a bulk crystal having dislocations and the theoretical break shear stress of the MC. They suggest reasonably that the metallic elements having the largest Poisson's ratio hold the largest MC-forming ability since such metals have the smallest elastic energy storage within the crystals and can thus endure the largest plastic deformation.

In this presentation, we show a straightforward approach to determining directly the length, strength, extensibility, and the thermal stability of the Au−MC as well as the binding energy of a core electron by decoding the measured size dependence of both the Au 4f level energy[21] and the melting-point suppression of Au nanosolids based on the recent bond-order-length-strength (BOLS) correlation mechanism.[22] Taking the effects of atomic coordination number (CN) imperfection, thermal expansion, and mechanical stretching extension into consideration, an analytical solution for the stretching limit of atomic distance in a metallic monatomic chain has been derived. Matching the calculated Au−Au stretching limit to all the insofar-measured values at various temperatures indicates that the scattered data arises from thermal and mechanical fluctuations and that the tendency of MC formation depends on the bulk melting point.

II. Theory

The striking difference between a bulk solid and a spherical nanosolid near the lower end of the size limit (a primary unit cell) is that the CN (or z_i) of the involved atom is reduced from 12 to 2 that is right the CN value of an atom in the MC. According to Goldschmidt[23] and Feibelman,[24] if an atom reduces its CN from 12 to 8, 6, 4, and 2, the radius of the specific atom will contract correspondingly by 3, 4, 12, and 30%. Such atomic−CN atomic-size correlation depends merely on atomic CN and it is independent of the nature of the bond. It is known that any spontaneous process is always accompanied with energy minimization. Therefore, the CN-imperfection-induced spontaneous bond contraction and the associated binding energy decrease (magnitude increase) enhance the bond energy density *per unit volume* in the relaxed surface region due to the unchanged bond number density. The CN imperfection also lowers the cohesive energy *per atom* in the surface region due to the reduced number of bond per atom. This leads to the BOLS correlation that is formulated as[2]

$$\begin{cases} c_i(z_i) = 2/[1 + \exp((12 - z_i)/8z_i)] = 0.6973 \quad (z_i = 2) \\ E_i(T = 0) = c_i^{-m} E(T = 0) \end{cases} \tag{1}$$

The bond contraction coefficient $c_i = d_i/d$ fits nicely the notations of Goldschmidt and Feibelman.[22] $E_i(T = 0)$ and $E(T = 0)$ are the maximal values of the interatomic potential.[25] Subscript i denotes the atom at the ith atomic layer and m an adjustable parameter depending on the nature of the bond involved. For pure metals, $m = 1$. The atomic CN changes with the curvature of the surface. For a flat or a slightly curved surface, $z_1 = 4$;[26] for a spherical dot, $z_1 = 4(1 - 0.75/K_j)$.[27] $z_2 = 6$ and $z_3 = 12$. $K_j = R_j/d$ is the number of atoms lined along the radius of the spherical dot.

Figure 1 illustrates schematically the BOLS correlation using the dimer interatomic potential. When the CN of an atom is reduced, the equilibrium atomic distance will contract from one (unit in d) to c_i and the bond energy of the remaining CNs will increase in magnitude from one (unit in $E_d = E(T = 0)$) to c_i^{-m}. The dotted and the solid $u(r)$ curves correspond to the interatomic potential of a dimer bond with and without atomic CN imperfection. The bond length−strength correlation herewith is consistent with the trend in ref 10 though the amounts of bond contraction and energy enhancement are different. The characteristic energies show that:

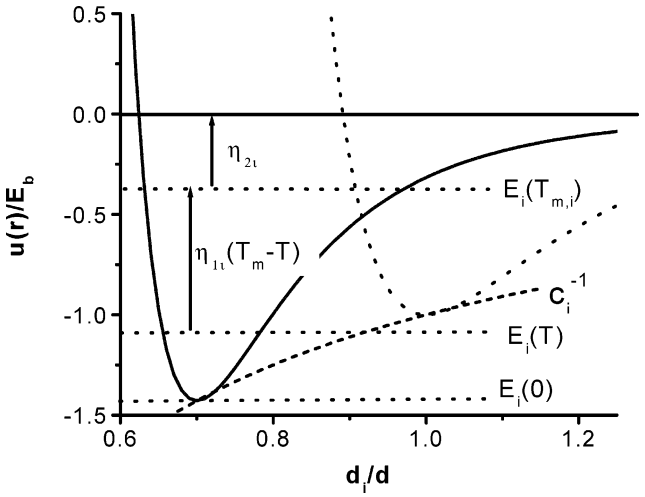

Figure 1. Schematic illustration of the BOLS correlation in a pairwise interatomic potential for a MC (solid curve) and for two atoms in the bulk (dotted curve). Atomic CN imperfection causes the bond to contract from 1 (unit in d) to 0.6973 and the cohesive energy per coordinate increases from 1 (E_b) to 1.43 by gliding the solid curve along the c_i^{-1} line to the solid curve. Separation between $E_i(T)$ and $E_i(0)$ is the thermal vibration energy. Separation between $E_i(T_{m,i})$ and $E_i(T)$ corresponds to energy that is needed for melting and contribute to mechanical strength. $T_{m,i}$ is the melting point. The energy required to break the bond at T is the separation between zero and $E_i(T)$. η_{2i} corresponds to the $1/z_i$ energy for atomization of a molten atom.

TABLE 1: Relation Between the Bond Energy and the Melting Point of Various Structures[a]

	fcc	bcc	diamond structure
η_{1b} (10^{-4} eV/K)	5.542	5.919	5.736
η_{2b} (eV)	−0.24	0.0364	1.29

[a] $E_b = \eta_{1b}T_m + \eta_{2b}$.[28]

(i) Separation between $E = 0$ and E_i(T) is the cohesive energy per CN at T, required for the bond breaking.

(ii) The spacing between $E_i(T)$ and $E_i(0)$ is the thermal vibration energy per coordinate.

(iii) $T_{m,i}$ being the melting point of the MC is proportional to the atomic cohesive energy, z_iE_i(at $T = 0$).[25]

If one wants to melt an atom with z_i coordinates by raising the temperature from T to $T_{m,i}$, one needs to provide energy

$$z_i[E_i(T_{m,i}) - E_i(T)] = z_i\eta_{1i}(T_{m,i} - T) \tag{2}$$

Breaking the bond mechanically at temperature T needs energy

$$\begin{aligned} 0 - E_i(T) &= \eta_{1i}(T_{m,i} - T) + \eta_{2i} \\ &= c_i^{-m}[\eta_{1b}(T_{m,b} - T) + \eta_{2b}] \end{aligned} \tag{3}$$

Ideally, the slope η_{1i} is an equivalent of specific heat per coordinate. The constant η_{2i} represents $1/z_i$ times energy that are required for evaporating a molten atom in the MC. η_{1i} and η_{2i} can be determined with the known c_i^{-m} and the η_{1b} and η_{2b} values for various structures as given in ref 28 and Table 1. Subscript b denotes bulk values.

The CN imperfection and the induced bond-energy rise contribute not only to the cohesive energy ($E_{coh,i} = z_i E_i$) of a single atom but also to the binding energy density ($E_{B,i} = n_i E_i$) in the relaxed region. The atomic $E_{coh,i}$ determines the thermodynamic behavior of a nanosolid such as melting or thermal rupture of a MC ($T_m \propto E_{coh}$).[25] By consideration of the contribution from temperature, the compressibility (under compressive stress) or extensibility (under tensile) at constant temperature is given by

$$\beta_i(z_i,T) = -\frac{\partial V}{V\partial P}\Big|_T = \left[-V\frac{\partial^2 u(r,T)}{V\partial V^2}\right]^{-1}\Big|_T \propto \frac{d^\tau}{N[E_i(T_{m,i}) - E_i(T)]} \propto \{n_i[E_i(T_{m,i}) - E_i(T)]\}^{-1} \propto \{n_i[\eta_{1i}(T_{m,i} - T)]\}^{-1}$$

where

$$P = -\frac{\partial u(r,T)}{\partial V}\Big|_T \tag{4}$$

β is in an inverse of Young's modulus or hardness in dimension that equals the sum of bond energy per unit volume.[29] N is the total number of bonds in d^τ volume. The $n_i = 2/d_i$ for linear extension consideration. Thus the temperature-dependent extensibility of a MC is calibrated with the bulk value at $T = 0$ as

$$\beta_i(z_i,T)/\beta_0(z_b,0) = \{n_b\eta_{1b}T_{m,b}/[n_i\eta_{1i}(T_{m,i} - T)]\} = \frac{\eta_{1b}d_i}{\eta_{1i}d}\left(\frac{T_{m,b}}{T_{m,i} - T}\right) \tag{5}$$

The term η_{2i} does not come into play, as the mechanical strength of a molten solid is almost zero.

As a scaling law, the measured size dependence of a $Q(R_j)$ is always proportional to the inverse R_j (and converges at $K_j < 3$) with a slope b. Combining measurement with theory,[25-27] we have

$$Q(R_j) - Q(\infty) = \begin{cases} bR_j^{-1} & (measurement) \\ Q(\infty)\Delta_{qj} & (theory) \end{cases} \tag{6}$$

with $Q(\infty) \equiv b/(\Delta_{qj}R_j)$. The $\Delta_{qj} \propto R_j^{-1}$ varies simply with the parameter m and the known dimensionality and size of the solid. There are only two independent variables, m and $Q(\infty)$. If a certain known $Q(\infty)$ value such as the $T_m(\infty)$ of the considered system is given, the m can be readily obtained. With the obtained m, any other unknown quantities $Q(\infty)$ such as the crystal binding intensity, $E_{4f}(\infty)$, of the same system then can be determined uniquely with the above relations. Not surprisingly, the size-and-shape dependence of a detectable quantity of the same system can also be predicted for materials design once the corresponding $q(z,E)$ function is established.

On the basis of the BOLS correlation, we have derived numerical expressions for the size-induced perturbation to the mean lattice constant (Δ_{d_j}) and Hamiltonian (Δ_{H_j}) that determine the core-level shift, band gap expansion, and atomic cohesive energy (Δ_{coh_j}) that determines the critical temperature for phase transition and melting point for a nanosolid.[25-29] Size and temperature perturbed compressibility/extensibility (Δ_{β_j}) has been derived here. Relations are summarized as follows

$$\begin{cases} \Delta_{d_j} = \sum_{i\le 3}\gamma_{ij}\dfrac{d_i - d}{d} = \sum_{i\le 3}\gamma_{ij}(c_i - 1) < 0 \\ \Delta_{H_j} = \sum_{i\le 3}\gamma_{ij}\dfrac{n_iE_i - n_bE}{n_bE} = \sum_{i\le 3}\gamma_{ij}(n_{ib}c_i^{-m} - 1) > 0 \\ \Delta_{coh_j} = \sum_{i\le 3}\gamma_{ij}\dfrac{z_iE_i - z_bE}{z_bE} = \sum_{i\le 3}\gamma_{ij}(z_{ib}c_i^{-m} - 1) < 0 \\ \Delta_{\beta_j} = \sum_{i\le 3}\gamma_{ij}\dfrac{d_i^\tau E_i^{-1} - d_0^\tau E^{-1}}{d_0^\tau E^{-1}} = \sum_{i\le 3}\gamma_{ij}(c_i^{\tau+m} - 1) < 0 \end{cases} \tag{7}$$

where E_i and E are the cohesive energy per CN at $T = 0$ K. $\gamma_{ij} = \tau c_i/K_j$ ($K_j = R_j/d$) is the volume ratio of the ith atomic layer to the entire solid of R_j radius. $\tau = 1$, 2, and 3 represents the dimensionality of a thin plate, a rod, and a spherical dot. One needs to note that the bond number density in the relaxed region does not change upon relaxation. For instance, bond relaxation never changes the bond number between the neighboring atoms in a MC ($\tau = 1$) whether it is suspended or embedded in the bulk. By incorporation of the above relations into the measured size-and-shape dependence of the corresponding properties, we can obtain quantitative information that is beyond direct measurement. For a spherical dot at the lower end of the size limit, $K_j = 1.5$ ($R_j = K_j d = 0.43$ nm for an Au spherical dot), $\gamma_{1j} = 1$, $\gamma_{2j} = \gamma_{3j} = 0$, and $z_1 = 2$, which is identical in situation to an atom in a MC despite the geometrical orientation of the two interatomic bonds. Actually, the bond orientation contributes not to the modeling iteration. Therefore, the performance of an atom in the smallest nanosolid is a mimic of an atom in a MC of the same element without presence of external stimulus such as stretching or heating.

By consideration of the effects of atomic CN-imperfection-induced bond contraction, thermal expansion (with linear coefficient α), and the temperature dependence of extensibility (with coefficient β), the distance between the two nearest atoms in the interior of a MC, under mechanical (P) and thermal (T) stimuli, can be expressed as

$$d_i(z_i,T,P) = dc(z_i)(1 + \alpha T)[1 + \beta_i(z_i,T)P]$$

or the maximal strain

$$\frac{\Delta d_i(z_i,T,P)}{d_i(z_i,T,0)} = \frac{d_i(z_i,T,P)}{d_i(z_i,T,0)} - 1 = \beta_i(z_i,T)\bar{P} \tag{8}$$

where $d_i(z_i,T,0) = dc(z_i)(1 + \alpha T)$ is the bond length at T without mechanical stress. At bulk melting point, the liner thermal expansion ($\alpha T_{m,b}$) is around 2% for most metals. On the other hand, mechanical rupture of a bond needs the $1/z_i$ times energy that is required for evaporating the specific ith atom, given in eq 3. Therefore

$$\int_{d_i(z_i,T,0)}^{d_i(z_i,T,P)} P dx = \bar{P}[d_i(z_i,T,P) - d_i(z_i,T,0)] = \bar{P}\Delta d_i = \eta_{1i}(T_{m,b} - T) + \eta_{2i} \tag{9}$$

One can approximate P to the mean $\bar{P}$ in eqs 8 and 9 if the $d_i(z_i,T,P)$ represents the breaking limit. As shown below, the analytical expression of the maximal strain is inapparently

TABLE 2: The Length and Energy of the Au−Au Bond in the Monatomic Chain and the Core-Level Energy of an Isolated Au Atom Obtained from Decoding the $E_{4f}(R_j)$ and $T_m(R_j)$ of Nanosolid Au

	Au/Octan	Au/TiO_2	Au/Pt	Au/Thiol
b	3.7804	1.5253		
m		1		
τ	3	1	1	3
E_{4f}(eV)	−81.504	−81.506	−81.504	−81.505
$\Delta E_{4f}(\infty)$(eV)	−2.866	−2.864	−2.866	−2.865
d_{MC} (nm)		0.2001		
$\epsilon_{MC}/\epsilon_{bulk}$		1.43		
$T_{m,MC}/T_m(\infty)$		1/4.2		

P dependent. The combination of eqs 4, 8, and 9 yields the maximal strain of a single bond in the MC

$$\frac{\Delta d_i(z_i,T,P)}{d_i(z_i,T,0)} = \{\beta_i(z_i,T)[\eta_{1i}(T_{m,i} - T) + \eta_{2i}]/d_i(z_i,T,0)\}^{1/2} = \left[\frac{\eta_{1b}\beta_0}{\eta_{1i}d}\left(\frac{T_{m,b}}{T_{m,i} - T}\right)[\eta_{1i}(T_{m,i} - T) + \eta_{2i}]\right]^{1/2} = \left[\frac{\beta_0\eta_{1b}T_{m,b}}{d}\left(1 + \frac{4.2\eta_{2i}/\eta_{1i}}{T_{m,b} - 4.2T}\right)\right]^{1/2} \cong \left(\frac{\beta_0\eta_{1b}T_{m,b}}{d}\right)^{1/2}\exp\left(\frac{2.1\eta_{2i}/\eta_{1i}}{T_{m,b} - 4.2T}\right) \quad (10)$$

Therefore, the maximal strain of a metallic MC depends on the temperature difference between the MC melting point and the measuring temperature, the magnitudes of the strain varies with materials bulk extensibility (at 0 K), bulk bond length, and the bulk melting point.

III. Results and Discussion

3.1. Au Nanosolid. *4f Core-Level Shift.* We may let $Q(\infty) = \Delta E_{4f}(\infty) = E_{4f}(\infty) - E_{4f}(1)$ in eq 6 for a Au solid to decode the measured size dependence of the core-level shift. Least-mean-square linearization of the measured $E_{4f}(1/R_j)$ of Au nanosolids deposited on an octanedithiol,[21] TiO_2[30] and Pt[31] substrate, and thiol-capped Au particles[32] gives intercept a that correspond to the bulk value of $E_{4f}(\infty) = -84.37$ eV,[33] and slopes b that vary with the dimensionality of the Au solids grown on different substrates. With the known $m = 1$ value for pure metals,[25] the $E_{4f}(\infty)$ and $E_{4f}(1)$ can be determined as given in Table 2.

Comparing the two theoretical curves for a spherical dot and a thin plate with the measured profiles in Figure 1a reveals that the Au solid on octanedithiol substrate follows ideally the curve of a spherical dot. It is also revealed that at $R = 1.5d = 0.43$ nm, the Au−Au distance contracts by ∼30% from 0.2878 to ∼0.2007 nm, which is close to the value 0.23 ± 0.04 nm, measured at 4.2 K[9] and the calculated shorter distance of 0.232 nm as well.[10] The cohesive energy per bond increases by ∼43%, which coincides with the measured E_{4f} from the smallest Au nanosolid as shown in Figure 2a. The deviation between theory and measurement from the thinner Au/TiO_2 film is due to the initial islandlike growth mode of metal on oxide surface[30,34] as well as the Au/TiO_2 interfacial effect. The Au−O bond forms at the interface, and the O−Au bond should be stronger than the Au−Au bond. Such bond nature alteration also strengthens the local crystal field and hence the core-level energy. Oxide bond formation generally causes the core level of the parent metal to shift up by 0.6−1.0 eV.[15,35] Measurements in Figure 2a show the interesting trend that the core level drops abruptly from that of an isolated atom by a maximum (∼40%) upon the MC being formed and then the shift recovers in a R^{-1} fashion to the bulk value when the solid grows from atomic scale to macroscopic size. At the thermal or mechanical rupture point of the MC, the core-level energy of the atom should approach to the original level of an isolated atom until the bond is completely broken according to the experimental and theoretical observations.

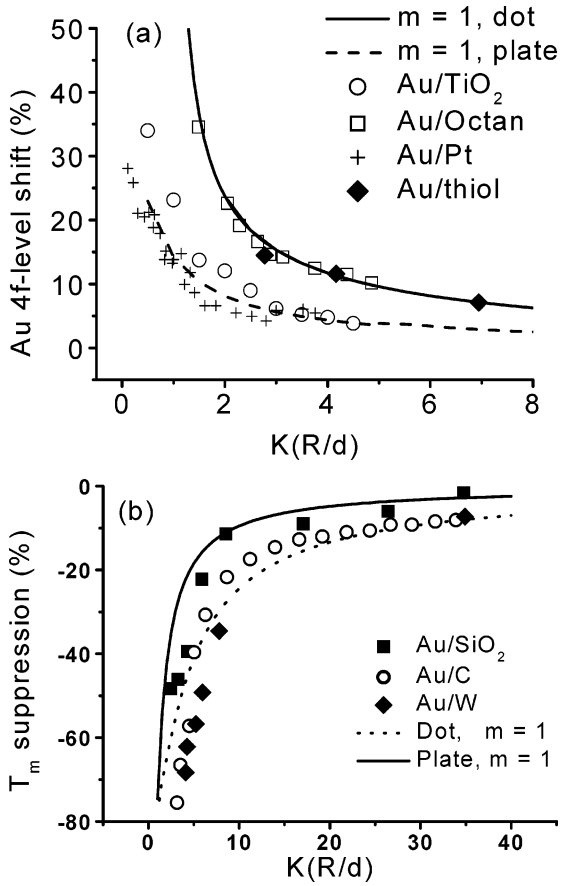

Figure 2. Comparison of theory with the measured size dependence of (a) $[E_{4f}(K) - E_{4f}(\infty)]/[E_{4f}(\infty) - E_{4f}(1)]$ of Au (nanodot) on octanedithiol[21] and Au (nanoplate) on TiO_2[30] and Pt[31] substrates and thiol-capped[32] with derived information as given in Table 2 and (b) $[T_m(K) - T_m(\infty)]/T_m(\infty)$ of Au nanosolids on W[36] and C[37] substrates and embedded in the SiO_2 matrix,[38] showing strongly interfacial effects and dimensionality transition on the Au nanosolid melting. $K = R/d$. Melting at the lower end of size limit ($K = 1.5$, $z = 2$) corresponds to the situation of a Au−MC.

Thermal Stability. Calibration with $Q(\infty) = T_m(\infty) = 1337.33$ K and by use of the same $m = 1$ value used in calculating the $E_{4f}(R_j)$, we obtained the theoretical T_m suppression curves for different shapes, which are compared in Figure 2b with the measured size-dependent T_m of Au on W[36] and on C[37] substrates and Au encapsulated in Silica matrix.[38] Differing from the core-level shift data, the melting profiles show that at the smaller size, the Au/W interface promotes more significantly the melting of Au (super cooling) than the Au/C interface. The silica matrix causes slightly superheating of the embedded Au solid compared with the other two substrates. Besides, the T_m measurement is a thermodynamic process that may affect the results to some extent. Nevertheless, the theoretically predicted melting curves merge at the lower end of the size limit, $K = 1.5$ with 75% suppression. Therefore, it is anticipated that thermal rupture of the Au−Au chain occurs at ∼320 K, much lower than the bulk melting point (1337.33 K).

Mechanical Strength. According to eq 7, the compressibility/extensibility of the MC at 0 K is 0.5 ($= 0.7^2 - 1$) times the

bulk values. The shortened bond is twice stronger (strength = $\epsilon_i/d_i \propto c_i^{-2} = 0.7^{-2} \approx 2$), agreeing with predictions of ref 12. This means that more force is required to stretch or compress a single bond in the MC by the same length compared to the force needed to stretch the same single bond in the bulk by the same amount, in general, whereas high-pressure X-ray diffraction revealed that the lattice constant of small alumina solid is easier to compress than larger ones.[39] This agrees with the current temperature dependence of the strain limit (eq 10) that varies with the drop of melting point of the nanosoild.

3.2. MC Forming and Breaking. Equation 10 indicates that a metallic MC melts at a temperature that is 1/4.2 times the bulk melting point. Therefore, an MC can hardly form at room temperature or above if the bulk T_m of the specific metal, such as Sn (505.1 K), Pb (600.6 K), and Zn (692.7 K), is below 300 × 4.2 = 1260 K. However, a Ti−MC with $T_{m,b} = 1941$ K may form at the 400−450 K range, slightly lower than the MC melting point $T_{m,i} = T_{m,b}/4.2 = 462$ K. The high extensibility is dominated in the temperature range that should correspond to the semisolid state. This may explain why some metallic MCs can form at ambient and some are not. This agrees with Jiang's prediction based on considerations of stress ratio.[20]

Applying $\alpha = 14.7 \times 10^{-6}$, $z_i = 2$, $z_b = 12$, $T_{m,b} = 1337.33$ K, $d = 0.2878$ nm, $d_i(0\ K) = 0.2007$ nm, and the measured mean $d_i(300\ K) = 0.31$ nm for an Au−MC to eq 10, $\beta_0 = 0.005\ GPa^{-1}$, $\eta_{2i}/\eta_{1i} = 64$ K were obtained. If $\eta_{1b} = 0.0005542$ eV/K and $\eta_{2b} = -0.24$ eV were taken from Table 1, $\eta_{1i} = 0.00187$ eV/K $\sim 3\eta_{1b}$, and $\eta_{2i} = 0.1197$ eV can be obtained. It is indicated that $\eta_{2b} < 0$ means that the energy required for breaking the bond for an atom in molten state is included in the term of $\eta_{1b}T_m$ and therefore the η_{1b} exaggerates the specific heat per CN. The accuracy of solutions is subject strictly to the η_{1b} and η_{2b} values and the precision of the measured $d_i(T \neq 0)$ in calculation. What one needs in calculation is the stretching limit measured at any two temperatures. The curve of temperature dependence of the stretching limits for an Au−MC, as shown in Figure 3, covers all the reported values measured at 4 K (0.23 ± 0.04 nm) and at ambient (298 ± 6 K, 0.29 ∼ 0.48 nm). Singularity appears at the $T_{m,i}$. In reality, any fluctuation of the T or the stretching force P in measurement will affect the measured value, and therefore, it is understandable now why the room-temperature Au−Au breaking limit varies from source to source.

3.3. Metallic Nanowires. Understanding may provide a complementary mechanism for the high ductility of metallic, such as Cu and Al, nanograined nanowires at room temperature or subambient.[40] Measurement results show that the detectable maximal strain of a suspended Au−MC bond is 0.48/0.2 − 1 = 140%, which is quite lower compared with the strain (10^3) of a nanograined Cu nanowire of several nanometers across.[41] Therefore, mechanism of atomic gliding dislocations and grain boundary movement would dominate the high ductility of nanowires.[1,40] The CN-imperfection-lowered atomic cohesive energy is suggested to be responsible for lowering the barrier or activation energy for atomic dislocation at the grain boundary of a nanosolid and the activation energy for chemical reaction, according to the current approach.

Figure 3b showing the z- and T-dependent maximal bond strain indicates that the melting of a nanosolid starts from the first surface shell and then the next when the temperature is raised. This agrees with the "liquid shell nucleation and growth" fashion[42] and the "surface phonon instability" models[43] for nanosolid melting. Figure 3b also suggests a possible mode for the stretched breaking of a defect-free nanowire. At a temperature close to the melting point, the maximal strain approaches infinity. Therefore, at temperatures around the melting point of the first shell and above, bond breaking under tension starts from the nanowire interior because the inner bonds reach their strain limits first. However, at temperatures much lower than the melting point of the first shell, bond breaking may start from the outermost atomic shell. Figure 3b shows that the maximal strains at low T for the surface shell is $\epsilon_3 < \epsilon_2 < \epsilon_1 < 15\%$. If one pulls the entire nanowire by xd per d length, the strain of the bonds in the respective shells will be $\epsilon_i = x/c_i$. Because $c_1 < c_2 < c_3$, then $\epsilon_3 > \epsilon_2 > \epsilon_1$, which is in an inverse order of the strain at low T, as shown in Figure 3b. Therefore, the breaking mode of a nanowire at low T is expected to be opposite to that at higher T. One needs to note that the bombardment of electron beams in the transition electron microscope will lower the melting point by hundreds of degrees depending on the beam energy[44] and the bond breaking will release energy that will raise the temperature of the atoms surrounding the broken bond. By use of a "nanostressing stage" located within a scanning electron microscope, the multiwalled carbon nanotubes were measured at room temperature to break in the outermost shell.[45] The "sword-in-sheath" failure agrees with the expectation of the current approach, and it is explained that the measuring temperature is far below the tube melting point of 1600 K or higher.[19] It is expected to be confirmed that the gold nanowire

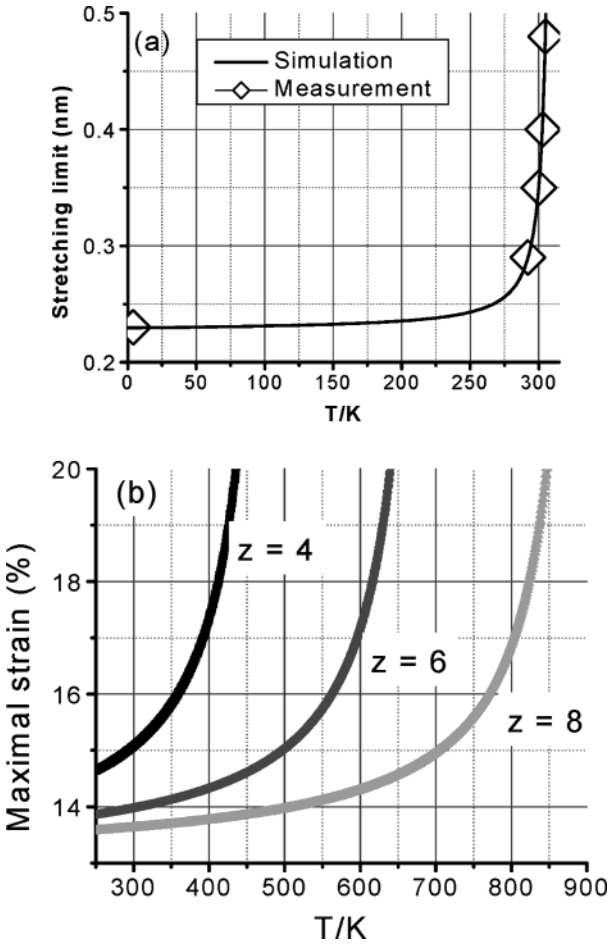

Figure 3. (a) Comparison of the theoretical curve with the breaking limit measured at 4 K (0.23 ± 0.04 nm) and at room temperature (298 ± 6 K, 0.29−0.48 nm), showing that the large range of the measured data arise from thermal fluctuation within 6 K. (b) Temperature and CN (z) dependence of the Au−Au bond maximal strain shows the order of melting at a curved surface and implies the breaking mode of a nanowire at different temperature range, see text.

breaking start from the inner shell as the measuring temperature is close to the outer-shell melting point of ∼450 K. It has been reported that the helical multishell gold nanowires[46] become thinner and thinner without breaking the outer-shell atomic bond.[47]

IV. Conclusion

The BOLS correlation mechanism has enabled us to calibrate the length, the strength, the extensibility, and the thermal stability of the Au−MC bond under the conditions with and without thermal and mechanical stimuli. The $E_{4f}(1)$ of an Au atom isolated from the solid and the crystal binding intensity, $\Delta E_{4f}(\infty)$, has been obtained by simultaneously simulating the measured size dependence of the $E_{4f}(R_j)$ and $T_m(R_j)$. Major findings are summarized as follows:

(i) Without external stimuli, the metallic bond in an MC contracts by ∼30%, associated with ∼43% magnitude rise of the bond energy.

(ii) The E_{4f} level energy of an isolated Au atom is −81.50 eV, and the bulk crystal binding energy to the 4f electrons is −2.87 eV. The binding energy increases by 43% when it forms a metallic MC or nanosolid at the lower end of the size limit, and then the binding energy drops to the bulk value when the solid increases its size. A metallic MC melts at 1/4.2 times the bulk melting point.

(iii) An analytical solution shows that the strain limit of a metallic bond in a MC under tension varies inapparently with mechanical stress but apparently with temperature in the form $\exp[A/(T_m - 4.2T)]$. This determines the tendency that a metallic MC forms or breaks and their temperature range.

(iv) Matching the calculated Au−Au distance to all the insofar-measured values indicates that the deviation in measurement originates from thermal and mechanical fluctuations and no light atom insertion is necessary.

Findings provide a consistent insight into the coordination-imperfection-enhanced binding intensity, mechanical strength, the suppressed thermal stability, and the compressibility/extensibility of a MC, which could be extended to the thermal and mechanical behavior of other metallic nanowires. The developed approach provides an effective way of determining the bulk 0 K extensibility, β_0, the effective specific heat η_{1i} per coordinate and the energy ($2\eta_{2i}$) required for evaporating an atom from the molten MC, provided with correct η_{1b} value. The effect of atomic CN imperfection and the temperature-dependent extensibility may need to be considered in sophisticated density functional theory calculations. Practice should be a helpful exercise for information of a MC bonding identities and the single electron energy of an isolated atom, one of the challenging tasks for nanometrology.

References and Notes

(1) Champion, Y.; Langlois, C.; Guerin-Mailly, S.; Langlois, P.; Bonnentien, J.-L.; Hytch, M. J. *Science* **2003**, *300*, 310.

(2) Sun, C. Q.; Tay, B. K.; Fu, Y. Q.; Li, S.; Chen, T. P.; Bai, H. L.; Jiang, E. Y. *J. Phys. Chem.* **2003**, *B107*, 411.

(3) Sun, C. Q. *Phys. Rev. B.* **2004**, *89*, 45105.

(4) Ohnishi, H.; Kondo, Y.; Takayanagi, K. *Nature* **1998**, *395*, 780.

(5) Rao, C. N. R.; Kulkarni, G. U.; Thomas, P. J.; Edwards, P. P. *Chem.−Eur. J.* **2002**, *8*, 29.

(6) Takai, Y.; Kadwasaki, T.; Kimura, Y.; Ikuta, T.; Shimizu, R. *Phys. Rev. Lett.* **2001**, *87*, 106105.

(7) Yanson, A. I.; Rubio-Bollinger, G.; van den Brom, H. E.; Agraït, N.; van Ruitenbeek, J. M. *Nature* **1998**, *395*, 783.

(8) Legoas, S. B.; Galvao, D. G.; Rodrigues, V.; Ugarte, D. *Phys. Rev. Lett.* **2002**, *88*, 076105.

(9) Untiedt, C.; Yanson, A. I.; Grande, R.; Rubio-Bollinger, G.; Agraït, N.; Vieira, S.; van Ruitenbeek, J. M. *Phys. Rev.* **2002**, *B66*, 085418.

(10) Bahn, S.; Jacobsen, K. W. *Phys. Rev. Lett.* **2001**, *87*, 266101.

(11) Sørensen, M. R.; Brandbyge, M.; Jacobsen, K. W. *Phys. Rev.* **1998**, *B57*, 3283. (b) Torres, J. A.; Tosatti, E.; Dal Corso, A.; Ecorcolessi, F.; Kohanoff, J. J.; Di Tolla, T. D.; Soler, J. M. *Surf. Sci.* **1999**, *426*, L441. (c) Sánchez-Portal, D.; Artacho, E.; Junquera, J.; Ordejón, P.; García, A.; Soler, J. M. *Phys. Rev. Lett.* **1999**, *83*, 3884. (d) Häkkinen, H.; Barnett, R. N.; Scherbakov, A. G.; Landman, U. *J. Phys. Chem.* **2000**, *B104*, 9063.

(12) Rubio-Bollinger, G.; Bahn, S. R.; Agraït, N.; Jacobsen, K. W.; Vieira S. *Phys. Rev. Lett.* **2001**, *87*, 026101.

(13) Novaes, F. D.; da Silva, A. J. R.; da Silva, E. Z.; Fazzio, A. *Phys. Rev. Lett.* **2003**, *90*, 036101.

(14) Fu, Y. Q.; Yan, B. B.; Loh, N. L.; Sun, C. Q.; Hing P. *Mater. Sci. Eng.* **2000**, *A282*, 38.

(15) Sun, C. Q. *Prog. Mater. Sci.* **2003**, *48*, 521.

(16) Lee, S.-B.; Robinson, L. A. W.; Teo, K. B. K.; Chhowalla, M.; Hasko, D. G.; Amaratunga, G. A. J.; Milne, W. I.; Ahmed, H. *J. Nanosci. Nanotechnol.* **2003**, *3*, 325.

(17) Zhang, Y.; Franklin, N. W.; Chen, R. J.; Dai, H. *Chem. Phys. Lett.* **2000**, *33*, 135.

(18) Ajayan, P. M.; Terrones, M.; de la Guardia, A.; Huc, V.; Grobert, N.; Wei, B. Q.; Lezec, H.; Ramanath, G.; Ebbesen T. W. *Science* **2002**, *296*, 705.

(19) Sun, C. Q.; Bai, H. L.; Tay, B. K.; Li, S.; Jiang, E. Y. *J. Phys. Chem. B* **2003**, *107*, 7544.

(20) Jiang, Q.; Zhao, M.; Li, J. C. *Appl. Surf. Sci.* **2003**, *206*, 331.

(21) Ohgi, T.; Fujita, D. *Phys. Rev.* **2002**, *B66*, 115410.

(22) Sun, C. Q.; Tay, B. K.; Zeng, X.; Li, S.; Chen, T. P.; Zhou, J.; Bai, H.; Jiang, E. Y. *J. Phys. Condens. Matt.* **2002**, *14*, 7781.

(23) Goldschmidt, V. M. *Ber. Deut. Chem. Ges.* **1927**, *60*, 1270.

(24) Feibelman, P. J. *Phys. Rev.* **1996**, *B53*, 13740.

(25) Sun, C. Q.; Wang, Y.; Tay, B. K.; Li, S.; Huang, H.; Zhang, Y. B. *J. Phys. Chem.* **2002**, *B106*, 10701.

(26) Pan, L. K.; Sun, C. Q.; Tay, B. K.; Chen, T. P.; Li, S. *J. Phys. Chem.* **2002**, *B106*, 11725.

(27) Sun, C. Q.; Pan, L. K.; Fu, Y. Q.; Tay, B. K.; Li, S. *J. Phys. Chem.* **2003**, *B107*, 5113.

(28) Nanda, K. K.; Sahu, S. N.; Behera, S. N. *Phys. Rev.* **2002**, *A66*, 013208.

(29) Sun, C. Q.; Tay, B. K.; Lau, S. P.; Sun, X. W.; Zeng, X. T.; Bai, H.; Liu, H.; Liu, Z. H.; Jiang, E. Y. *J. Appl. Phys.* **2001**, *90*, 2615.

(30) Howard, A.; Clark, D. N. S.; Mitchell, C. E. J.; Egdell, R. G.; Dhanak, V. R.; *Surf. Sci.* **2002**, *518*, 210.

(31) Salmon, M.; Ferrer, S.; Jazzar M.; Somojai, G. A. *Phys. Rev.* **1998**, *B28*, 1158.

(32) Zhang, P.; Sham T. K. *Phys. Rev. Lett.* **2003**, *90*, 245502.

(33) Doniach, S.; Sunjic, M. *J. Phys.* **1970**, *4*, C31, 285.

(34) Becker, C.; Rosenhahn, A.; Wiltner, A.; von Bergmann, K.; Schneider, J.; Pervan, P.; Milun, M.; Kralj, M.; Wandelt, K. *New J. Phys.* **2002**, *4*, 75.

(35) Sun, C. Q.; Pan, L. K.; Bai, H. L.; Li, Z. Q.; Wu, P.; Jiang E. Y. *Acta Mater.* **2003**, *51*, 4631.

(36) Castro, T.; Reifenberguer, R.; Choi, E.; Andres, R. P. *Phys. Rev.* **1990**, *B42*, 8548.

(37) Buffat, Ph.; Borel, J. P. *Phys. Rev.* **1976**, *A13*, 2287.

(38) Dick, K.; Dhanasekaran, T.; Zhang, Z.; Meisel, D. *J. Am. Chem. Soc.* **2002**, *124*, 2312.

(39) Chen, B.; Penwell, D.; Benedetti, L. R.; Jeanloz, R.; Kruger, M. B. *Phys. Rev.* **2002**, *B66*, 144101.

(40) Lu, L.; Sui, M. L.; Lu, K. *Science* **2000**, *287*, 1463. (b) Wang, Y. M.; Ma, E.; Chen, M. W. *Appl. Phys. Lett.* **2002**, *80*, 2395.

(41) Valiev, R. Z.; Islamgaliev, R. K.; Alexandrov I. V. *Prog. Mater. Sci.* **2000**, *45*, 103.

(42) Reiss, H.; Wilson, I. B. *Colloid, J.* 1948, *3*, 551. (b) Sakai, H. *Surf. Sci.* **1996**, *351*, 285. (c) Ubbelohde, A. R. *The molten State of Matter*; Wiley: New York, 1978. (d) Wronski, C. R. M. *J. Appl. Phys.* **1967**, *18*, 1731. (e) Hanszen, K. J. *Z. Phys.* **1960**, *157*, 523.

(43) Jiang, Q.; Shi, H. X.; Zhao, M. *J. Chem. Phys.* **1999**, *111*, 2176. (b) Wautelet, M. *J. Phys. D: Appl. Phys.* **1991**, *24*, 343.

(44) Terrones, M.; Terrones, H.; Banhart, F.; Charlier, J. C.; Ajayan, P. M. *Science* **2000**, *288*, 1226.

(45) Yu, M. F.; Lourie, O.; Dyer, M. J.; Moloni, K.; Kelly, T. F.; Ruoff, R. S. *Science* **2000**, *287*, 637.

(46) Kondo, Y.; Takayanagi, K. *Science* **2000**, *289*, 606.

(47) Takayanagi, K. Private communication, Singapore, 1998.